Correlation of the vortex order-disorder transition with the symmetry of the crystal lattice in V_3Si

H. Küpfer,[1,2] G. Linker,[1] G. Ravikumar,[3] Th. Wolf,[1] A. Will,[4] A. A. Zhukov,[5] R. Meier-Hirmer,[1] B. Obst,[4] and H. Wühl[4,2]
[1]*Forschungszentrum Karlsruhe, Institut für Festkörperphysik, Postfach 3640, 76021 Karlsruhe, Germany*
[2]*Universität Karlsruhe, Fakultät für Physik, 76131 Karlsruhe, Germany*
[3]*Technical Physics and Prototype Engineering Division, Bhabha Atomic Research Centre, Mumbai-400085, India*
[4]*Forschungszentrum Karlsruhe, Institut für Technische Physik, Postfach 3640, 76021 Karlsruhe, Germany*
[5]*Department of Physics and Astronomy, Southampton University, Southampton, SO17 1BJ, United Kingdom*
(Received 30 September 2002; revised manuscript received 16 December 2002; published 28 February 2003)

The transitions from the ordered Bragg glass into the disordered vortex states at low and high fields are investigated by magnetization measurements varying the angle between magnetic field and crystal lattice orientations in a distinct manner. A single crystalline sphere is used to obtain an uniform demagnetization and not to introduce vortex disorder from sample edges. No angular dependence was observed when the pinning energy dominates. However, if the elastic energy of the vortex lattice is superior, the formation of the Bragg glass depends strongly on the relative orientation of both lattices. If the sphere is rotated around the [100] direction of the crystal with the field being perpendicular to it, a fourfold symmetry, both of the transition fields and of the strength of the vortex metastability, is found. The recent observation by Yethiraj *et al.* [Phys. Rev. Lett. **82**, 5112 (1999)], that the vortex lattice reflects the symmetry of the crystal lattice also in V_3Si is in good agreement with our investigations. Comparative measurements made on the sphere and on a crystal with edges revealed the influence of disorder on the Bragg glass induced by the sample shape.

DOI: 10.1103/PhysRevB.67.064507 PACS number(s): 74.25.Dw, 74.25.Qt, 74.70.Ad

I. INTRODUCTION

The transition of the vortex matter from the quasiordered Bragg glass phase (BG) into the disordered state or vortex glass (VG) is a topic of considerable interest in the vortex phase diagram of low and high T_c superconductors. In addition to this high-field order-disorder (HF-O/D) transition, the BG undergoes at low fields another transition into an amorphous or disordered state (LF-O/D) when the intervortex distance becomes comparable to the London penetration depth. Both transitions—related to the balance between elastic energy of the vortex lattice (E_{el}) and the pinning energy (E_p) (Refs. 1–4)—are expected to be of first order.[5–7] They are accompanied by vortex state metastability and magnetic history effects, well known for the HF-O/D transition,[8–13] and recently also found for the LF-O/D one in $NdBa_2Cu_3O_7$ and V_3Si.[14] The low-T_c superconductor V_3Si has a high Ginzburg Landau parameter κ, a very small anisotropy, and is in the clean limit. Its pinning energy can be tuned by fast neutron irradiation and subsequent thermal annealing[15–17] allowing a considerable variation of the field region where the BG is established. Based on these properties our studies have focused on the vortex phase diagram and related effects in V_3Si and on the comparison with results obtained from high-T_c superconductors.

In an ideal type-II superconductor the structure of the BG phase is expected to be a triangular lattice due to a repulsive interaction between vortices. Other structures of the vortex state have been observed in cubic single crystals of low-T_c and low-κ superconductors at low fields. Depending on the crystal orientation relative to the applied magnetic field the vortex state may have a twofold-, threefold-, or fourfold symmetry, and its orientation is locked to the crystal lattice in a unique manner.[18] Such a correlation between the two lattices was expected to be unimportant for high-κ materials. However, in previous investigations of the vortex lattice in cubic rare-earth nickel borocarbides square lattices and transitions between square and hexagonal lattices have also been found in these superconductors.[19] Recently, Yethiraj *et al.*[20] observed, in V_3Si by small-angle neutron scattering, that for a certain orientation of both lattices the hexagonal vortex lattice transforms into a square lattice in an increasing field. This is partly in accordance with predictions of theoretical calculations.[21] If the formation of different vortex lattice configurations depends on the symmetry of the crystal lattice in the direction of the applied field, it is natural to expect that the HF-O/D and LF-O/D transitions also show such an angular dependence. The main purpose of this paper is to investigate if such a correlation exists by measuring the angular dependence of both order/disorder transition fields on the crystal orientation (Sec III A). Magnetic history effects, related to ''superheating'' and ''supercooling'' of the BG and the disordered states, in the low- and high-field transitions, and their correlation with the crystal symmetry, are discussed in Sec III B. In Sec III C it is shown that this interaction between vortex and crystal lattices is only modified but not destroyed by the influence of vortex disorder induced into the BG by macroscopic edges of the sample shape.

II. EXPERIMENTAL

Stoichiometric V_3Si was prepared by repeated arc melting and subsequent homogenization at about 1800 °C under 0.5 bar argon pressure for three weeks. Grain growth from this treatment, which also dissolves V_5Si_3 precipitates, results in grain sizes up to 1 cm. A part of this material was irradiated with fast neutrons to a fluence of 10^{18} cm^{-2} (neutron energy above 1 MeV) at 40 °C. At this irradiation temperature the radiation-induced primary defect cascades reformed into stable, small point defect clusters. From the material before and after irradiation, spheres of 1.8 mm in diameter were prepared by the spark-cutting technique, and then chemically

etched and polished in order to remove the damaged surface. From these samples as well as from broken fragments single crystals were selected by x-ray measurements and the [100], [110], and [111] crystal directions were determined. A more detailed description of preparation, irradiation, and annealing was given in Refs. 15–17.

The magnetization was measured with a vibrating sample magnetometer (Oxford Instruments) where the sample can be rotated in a plane perpendicular to the applied magnetic field up to 7 T. The misalignment between the field direction and a specific crystallographic axis around which the sample should rotate was in the range of 2° to 10° because different sample holders were used in the x-ray and magnetization equipments. At each angle the magnetization $m(B)$ was measured with a constant sweeprate of the magnetic field of 10^{-2} T/s. After each measurement of the magnetization the angle was changed to the next position; then the field was cycled to a large negative value in order to erase the irreversible magnetic prehistory before the next magnetization loop was recorded.

We discuss measurements made on a sphere (S) and on an irregularity shaped, broken piece (P), both single crystalline, from the same arc-melted ingot prepared by the same procedure. After homogenization, but before irradiation, both samples (SO and PO) are characterized by the residual resistivity ratio $R=42$, the transition temperature $T_c=16.49$ K, the transition width $\Delta T_c=100$ mK, and a κ value of 17. At 13.3 K, where the upper critical field B_{c2} is close to 7 T, the BG extends without a HF-O/D transition up to the vortex liquid state. The same samples after irradiation (SI and PI) have $R=11$, $T_c=16.11$ K, $\Delta T_c=280$ mK, $\kappa=24$, and very high current densities which prevent the formation of the BG throughout the B, T plane. In order to decrease the pinning energy to a value, where the HF-O/D transition occurs and is experimentally accessible, the samples were annealed for 2 h at 630 °C. In this state (SA and PA) the parameters changed to $R=16$, $T_c=16.37$ K, $\Delta T_c=320$ mK, $\kappa=21$, and the HF-O/D transition is at about 3.5 T at a temperature of 13.3 K where the upper critical field reaches 6.7 T.

III. RESULTS AND DISCUSSION

A. Formation of the Bragg glass and the symmetry between vortex and crystal lattice

Figure 1 shows a comparison of $m(B)$ obtained from the same V_3Si sphere but with quite different values of E_p. The measurements are made at temperatures such that B_{c2} has the same value. The magnetization of the sphere before irradiation (SO) at 13.3 K is reversible above 0.5 T, corresponding to a current density $j<5$ A/cm^2. After irradiation the current density of the sphere (SI) at 1 T and 13.3 K is 6×10^4 A/cm^2; the sharp spikes in $m(B)$ result from flux jumps. At 1 T and 13.3 K the annealed sphere (SA) in the BG phase has about 10^2 A/cm^2 and 5×10^3 A/cm^2 in the peak region at 5 T. It is reversible in intermediate fields from 1.6 to 3.2 T. Fast neutron irradiation at room temperature induces small clusters of pointlike defects which are isotropic and randomly distributed. The isotropy of this defect structure is demonstrated by measuring magnetization loops in SI with

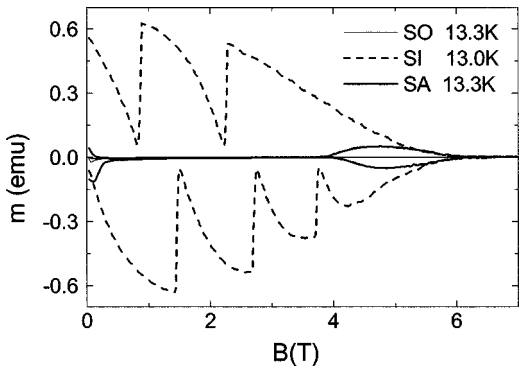

FIG. 1. Magnetization $m(B)$ of the V_3Si sphere after homogenization (SO), fast neutron irradiation (SI), and partial annealing (SA), measured at a temperature, which corresponds to the same upper critical field.

the angle Φ between the applied field and crystallographic orientation as a parameter. As an example, Fig. 2 shows $m(B)$ at four angles which differ by 45° when the sphere is rotated around the [100] direction and the field is perpendicular to the rotation axis (inset in Fig. 2). Also, any other rotation gives the same $m(B)$ within 10% as shown in Fig. 2. Such an isotropic behavior, which results from the random defect structure and the low superconducting anisotropy, is also expected in sample SA. But the experimental observation is quite the opposite. When the vortex matter is in the BG state the magnetization becomes strongly Φ dependent. In Fig. 3 the current density $j\sim\Delta m$ is plotted vs B with the angle Φ as a parameter. The gray area covers all $j(B)$ values obtained from magnetization at different angles at 13.3 K. This angular dependence disappears in the VG above the peak field ($B>5$ T) as well as in the amorphous state at low fields ($B<0.5$ T). The small angular dependence in these two field regions on either side of the BG is accounted for by the anisotropy of B_{c2}. But in the BG with $E_{el}>E_p$ the irreversibility varies with Φ by more than two orders of magnitude. At certain angles a reversible behavior may be observed in a wide field range between 1.4 and 3.4 T, whereas at other angles the current density is above 10^3 A/cm^2 in this field region. This extraordinary angular dependence of the

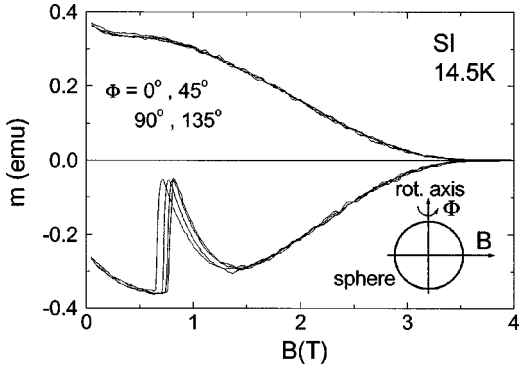

FIG. 2. Magnetization $m(B)$ of the V_3Si sphere after fast neutron irradiation at different angles Φ between the crystal orientation and magnetic field B. The rotation axis is parallel to the [100] direction of the crystal.

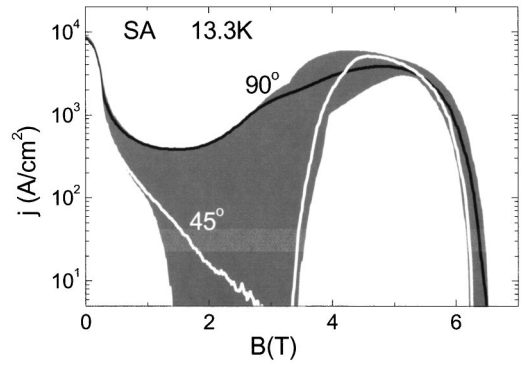

FIG. 3. Current density $j(B)$ of the V_3Si sphere after annealing, measured at different angles Φ between crystal orientation and magnetic field B. The gray area covers $j(B)$ from all possible variations of Φ. If the rotation axis is parallel to the [100] direction of the crystal and B along [010], $j(B)$ is given by the black line ($\Phi = 90°$), whereas the white line corresponds to $j(B)$ for B parallel to the [011] direction ($\Phi = 45°$).

magnetization is unlikely to result from an amorphous vortex phase introduced by the sample edges because the studied sample was a single crystalline sphere with an isotropic defect structure and a small superconducting anisotropy of about 5%. Among all $j(B)$ curves two have a very different shape (thick lines in Fig. 3). They are obtained for a rotation axis parallel to the [100] direction and B parallel to the [010] ($\Phi = 90°$, black line) or to the [011] direction of the crystal ($\Phi = 45°$, white line). The corresponding magnetization curves, shown in Fig. 4., differ considerably with respect to the width Δm in the BG region but are very similar in the VG above the peak field B_p and at fields below 0.5 T. We can, therefore, also exclude the presence of any macroscopic defects of preferred orientation as an origin for the observed behavior. Magnetization curves obtained between these two specific angles or/and for different rotation axes show the familiar shape of the well-known peak effect ($\Phi = 67°$; dashed line in Fig. 4). To quantify the field width where the BG exists, we define the transition field B_{HF} of the HF-O/D transition as the point of intersection from a linear extrapolation of m in increasing field (thin lines at 67° in Fig. 4).

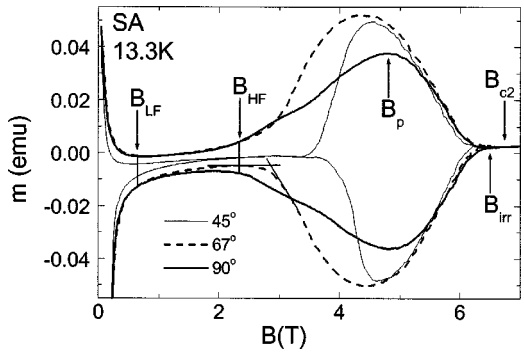

FIG. 4. Magnetization $m(B)$ of the V_3Si sphere after annealing with the angle Φ between crystal orientation and magnetic field B as parameter. $\Phi = 45°$ corresponds to B parallel to the [011], and $\Phi = 90°$ to B parallel to the [010] crystal direction.

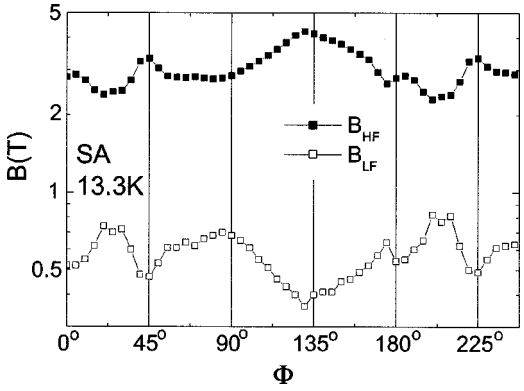

FIG. 5. Angular dependence of the high- and low-field order/disorder transition B_{HF} and B_{LF}, respectively, of the V_3Si sphere after annealing.

This determination becomes difficult if the transition in $m(B)$ is more gradual, and in particular for the determination of the transition field B_{LF} of the LF-O/D transition. For consistency, we therefore choose a Δm or current criterion which gave, for a sharp $m(B)$ transition, about the same field as obtained from the intersection point. This procedure, used for the determination of both transition fields at a temperature of 13.3 K, results in a current criterion of about 600 A/cm^2 (vertical lines in Fig. 4) corresponding to 10^{-5} part of the depairing current density. The irreversibility field B_{irr} was obtained from an extrapolated current criterion of 1 A/cm^2, and B_{c2} is that field at which $m(B)$ becomes paramagnetic in the normal state. These five characteristic fields—marked by arrows in Fig. 4 for $m(B, \Phi = 90°)$—are determined from one magnetization measurement at a constant angle Φ, as explained in Sec. II. For instance, the two transition fields B_{HF} and B_{LF} vs Φ are shown in Fig. 5. We note the opposite angular dependences of B_{LF} and B_{HF} which are responsible for the different extent of the BG region varying by more than a factor of 2 with Φ.

The characteristic fields in Fig. 5 have angular dependences with a twofold symmetry for the field applied parallel and antiparallel to the sphere because the rotation axis was not directed into a crystallographic orientation of high symmetry. If, however, the rotation axis is within the [100] direction, the angular dependences show a clear fourfold symmetry (Fig. 6). There are pronounced maxima of B_{HF} correlated with minima of B_{LF} if the field direction is parallel to the diagonal of the area of the unit cell [$\Phi = 45°$, 135°, and 225° in Figs. 6(a) and 6(b)], whereas in between and especially for B parallel to the edge of the unit cell ($\Phi = 0°$, 90°, and 180°) the extension of the BG is strongly reduced. In Fig. 6(a) the HF-O/D transition fields from the point of intersection (open squares) are plotted with those obtained from the current criterion (filled squares) for comparison. Deviations from an exact fourfold symmetry as seen by comparing the data at 90° and 180° are attributed to angular misalignments of the sphere with respect to the applied field. The fourfold symmetry is also observed in the angular dependences of B_{irr} and B_{c2} as shown in Fig. 6(c). They vary by about 5% corresponding to the superconducting anisotropy which is, as well as the maxima of B_{c2} for the field

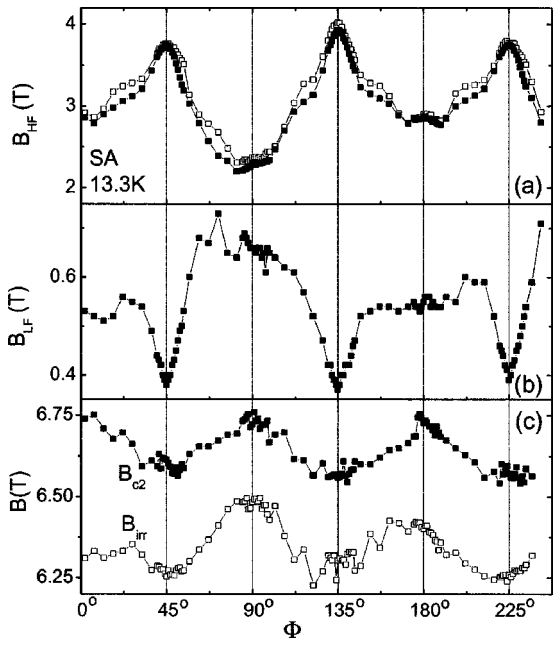

FIG. 6. Angular dependences of the high- and low-field order/disorder transitions B_{HF} (a) and B_{LF} (b), respectively, and of the upper critical field B_{c2} and irreversibility field B_{irr} (c) of the V_3Si sphere after annealing. The rotation axis is parallel to the [100] direction of the crystal, $\Phi = 45°$ corresponds to B parallel to the [011], and $\Phi = 90°$ to B parallel to the [010] crystal direction.

parallel to the [100] directions, in accordance with other measurements.[22] The error in the determination of these two fields is larger than that for B_{LF} and B_{HF}. If the rotation axis is parallel to the space diagonal of the unit cell (the [111] direction), the angular dependences of the transition fields show a sixfold symmetry: a threefold symmetry from the cubic crystal structure and a twofold symmetry from the applied field. The variations of both transition values with Φ are smaller than in the geometry discussed above, and the influence of misalignments is larger.

The above magnetization measurements at different angles between an applied magnetic field and a crystal lattice orientation revealed a pronounced angular dependence of the BG properties and the transition fields. In the BG region the elastic energy of the vortex lattice is the dominating energy scale, and the transitions into the disordered states at both boundaries are given by the balance between E_{el} and E_p. The small changes of these energies resulting from the small anisotropy of the superconducting parameters, such as $B_{c2}(\Phi)$ [Fig. 6(c)] or $\kappa(\Phi)$, cannot account for the strong angular dependence of the BG properties. The pinning energy, dominating in the disordered vortex states above B_{HF} and below B_{LF}, can also be excluded to be responsible because its angular dependence is moderate [$j(B,\Phi)$ in Fig. 3]. The elastic energy dominating in the BG phase results in a current density which varies by more than a factor of 10^2. Within the framework of the collective pinning theory[23,24] this requires a change of the correlation volume by 10^4, a factor which cannot be obtained from 5% anisotropy. This implies that—in addition to the anisotropy—E_{el} depends on the crystal direction; for example, it is larger for B parallel to the [011] ($\Phi = 45°$) than to the [010] direction ($\Phi = 90°$). A correlation between the vortex and crystal lattice symmetry in high-κ cubic superconductors from nonlocal effects was predicted by Kogan *et al.*[21] and partly experimentally verified in V_3Si by Yethiraj *et al.* [20] They observed that the vortex lattice transforms at 1 T and 1.8 K from triangular at low to square symmetry at high fields, but only if the field is parallel to the [100] direction. In fields along [110] the triangular lattice becomes distorted with increasing field but does not change its symmetry. When the transformation field of 1 T at B parallel to [100] and 1.8 K follows the usual temperature dependence $[1-(T/T_c)^2]$, it falls below 0.3 T at 13.3 K and therefore the triangular/square lattice transition should be without direct relevance for our observations. From this consideration we expect for our measurements at 13.3 K in the BG phase a square lattice at B parallel to [010] and an hexagonal lattice outside this direction. This is based on the assumptions that possible differences of crystal purity and pinning energy as well as the different preparations of the vortex lattice (field cooled in Ref. 20, and field swept in this work) are of minor importance for the transition. The gradual change of the magnetization between both principal directions does not allow one to determine the angle where the expected transition between hexagonal and square lattices occurs.

It then remains that the correlation of the vortex with the crystal lattice symmetry is the most probable origin of the angular dependence of the BG formation. The characteristic different behavior of the BG in the field parallel to the [010] direction of the crystal is related to properties of the square lattice different from the hexagonal one. The corresponding continuous HF-O/D transition and the much larger irreversibility below may be related to an impeded formation of a square lattice resulting from a swept field and the larger influence of quenched disorder.

The pronounced metastable behavior of the vortex matter in the BG phase—discussed in Sec. III B—offers an alternative explanation for the strong angular dependence of the BG properties. The correlation of the vortex with the crystal lattice symmetry may influence E_{el}, but is not so strong as to become the main origin as assumed in the explanation given above based on vortex configurations in the stable state. When vortices enter the sample along different crystallographic directions the degree of the introduced metastable phase for instance disordered phase in the stable BG region, as well as the time constant for annealing metastability, may be different. Because the experimental time scale is not long enough to measure the stable vortex state, all BG properties including the transition fields may be influenced by angular dependent metastability.

B. Magnetic history effects

The order/disorder transformation from the BG into the VG at B_{HF} is expected to be a first-order transition.[5,6,7,12] This is consistent with metastability of the vortex matter investigated by magnetic history effects (HEs) in this B, T area as already found and discussed in V_3Si.[14,25,26] The existence of HEs observed recently in the complementary area at the

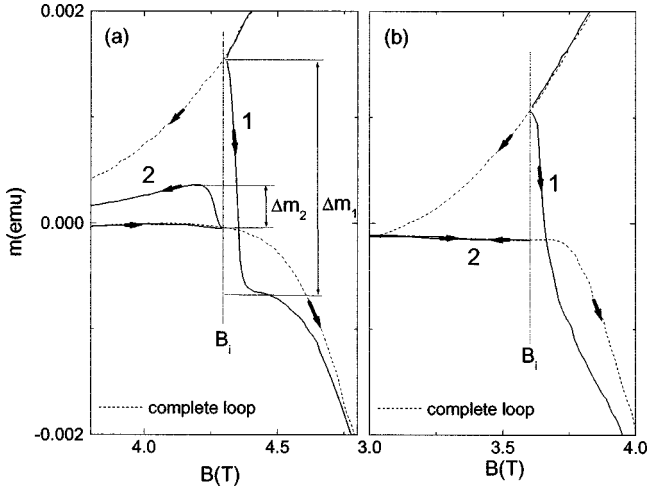

FIG. 7. (a) and (b) Magnetic history dependence of the high-field order/disorder transition of the V_3Si sphere after annealing. Partial loop 1 starts in the disordered and loop 2 in the ordered state, both are inverted at B_i. The ratio of the Δm values at B_i reflects the strength of metastability.

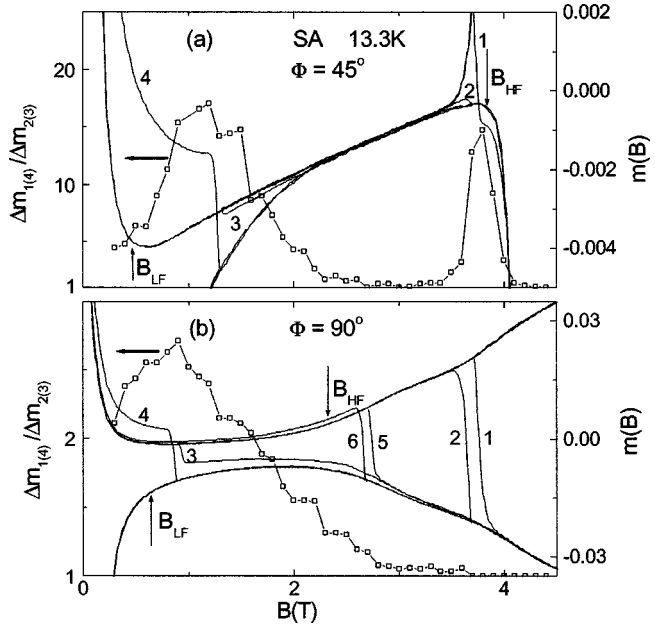

FIG. 8. Strength of the magnetic history dependence of the high-field ($\Delta m_1/\Delta m_2$) and low-field ($\Delta m_4/\Delta m_3$) order/disorder transitions and the corresponding magnetization loops (right axis) of the V_3Si sphere after annealing. (a) corresponds to the geometry magnetic field parallel to the [011], and (b) parallel to the [010] direction of the crystal.

low-field transition B_{LF} (Ref. 14) is not a proof of a first-order transition at low fields but supports it. We favor this possibility in comparison to a continuous transition based on plasticity, and discuss the metastability originating from a first-order transition both at low and high fields. Alternative possibilities for the HF-O/D transition were discussed by Chaudhary *et al.*[26]

The HE is investigated by comparing partial magnetization with the complete loop[11] [Fig. 7(a)]. The partial loop (1) starts in the disordered state at fields above B_p, and becomes reversed at a field B_i. After a field distance required for inverting the flux gradient, the loop shows an overshoot of m in comparison with the ascending branch of the complete loop (dashed line) if the amount of disordered vortex matter is larger than in the complete loop. On the other hand, if the partial loop (2) starts at negative fields or in the BG, and is reversed at B_i, an undershoot is observed if the amount of the ordered vortex phase is larger than in the descending branch of the complete loop. At the LF-O/D transition a larger amount of disordered vortex matter results in an overshoot for descending fields, and vice versa. A comparison between full and partial loop with B_i in the BG reflects the amount of metastable disordered phase whereas with B_i outside the BG the amount of metastable ordered in the stable disordered phase is probed. The ratio of the Δm values from both partial loops, as shown by the thin lines in Fig. 7(a) serves as a relative measure of the strength of the HE. This value, $\Delta m_1/\Delta m_2$, is the ratio of the current densities at B_i arising from the disordered and ordered states, respectively. The ratio is 1 if no HE is present, and is infinite if the partial loop 2 is reversible at B_i, as shown for example in Fig. 7(b). In this case, where B_i is situated in a reversible field region, the subsequent transition into the VG is not assisted or forced by the disordered phase which may be dragged from the amorphous low-field state, as shown in Ref. 14. This means that the transition field B_{HF}, obtained from a linear extrapolation of the complete loop in an increasing field, is equal to or—if ''superheating'' of the BG occurs—above the thermodynamic transition.

From the dependence of the vortex lattice formation on the symmetry of the crystal lattice, discussed in Sec. III A, the accompanying HE is also expected to be angular dependent. In Figs. 8(a) and 8(b) the HE for the two characteristically different geometries is shown. The position marked by $\Phi = 45°$ in Fig. 8(a) deviates by some degrees from this orientation of high symmetry in order to avoid reversible behavior in the BG which prevents the determination of the strength of the HE. Both ratios, $\Delta m_1/\Delta m_2$ for the HE, at B_{HF} and $\Delta m_4/\Delta m_3$ for the HE at B_{LF}, are extraordinarily high and comparable to each other, an unexpected finding because usually this factor is below 10 and the low-field HE is much less pronounced or even hardly observed. In the BG where the strength approaches 1, the HE changes from the high- to the low-field behavior, and vanishes in between. When the angle tilts away from $\Phi = 45°$, both HEs become less pronounced: the low-field HE extends to higher field values and is less suppressed, such that at 90° the high-field HE has vanished and the strength of the low-field HE decreased by about one order of magnitude [Fig. 8(b)]. A vanishing HE is not proof that the nature of the transition has changed, but together with the very gradual transformation of $m(B)$ in comparison to $\Phi = 45°$, the high-field transition seems to be continuous at 90° rather than of first order.

From the expected square lattice at $\Phi = 90°$, favored by the fourfold symmetry of a single vortex in this geometry,[21] we speculate that the formation of the square lattice in the presence of quenched disorder by a swept magnetic field

becomes more difficult than for a hexagonal lattice—a square lattice may be better pinned. This prevents a sudden transformation from a VG into a BG, and causes the larger irreversibility there. Besides the absence of the high-field HE another peculiarity is the extension of the low-field HE into the high field disordered state [Fig. 8(b)]. Partial loops started in the low-field disordered region (2,4,6) are never below the descending branch, and those from high fields (1,3,5) are never above the ascending branch of the complete loop after the field is inverted. This requires that partial loops coming from low fields carry much more metastable disordered vortex matter into the ordered state than those coming from high fields, which means that the high-field HE becomes buried by the low-field one. The excess of metastable disordered phases in the ascending field of the BG is proved by repeatedly cycling small minor loops which anneal the disorder.[14,27] After a large number of cycles starting from the forward curve, the width of the minor loops collapses and come close to the reverse curve. The opposite case may occur if the dragged disorder in descending fields from the VG is dominating, i.e., high- and low-field HEs can influence and reduce each other if the BG phase in between is not in the equilibrium state. Summarizing, the metastable behavior of the vortex matter in the sphere is very pronounced at both transitions if the BG becomes reversible in between. In a special geometry—field parallel to [010]—the high-field HE vanishes because the low-field disorder in the ascending branch extends into the VG, which may also prevent a first-order transition there. These observations support that metastability from ''superheating'' and ''supercooling'' is accompanied by the amount of the disordered vortex phase in the stable BG from the preceding order/disorder transition.

C. Edge contamination and the Bragg glass formation

Demagnetization, surface barriers, and edges of a sample influence or may even determine flux penetration, its distribution, and the position and sharpness of the BG/VG transition.[6,28] Edges may contribute in two ways: (i) through the existence of the superconducting boundary, and (ii) from sharp macroscopic edges of the sample. These regions where vortices are preferentially created and annihilated serve as a source of amorphous or highly disordered vortex matter which spreads into the bulk and contaminates the BG partly with disorder. In this subsection we discuss the influence of macroscopic edges of the crystal shape on the formation of the BG by comparing the results from the sphere (Secs III A and III B) with those from a piece broken from the same crystal the sphere is made from. The superconducting boundary and possible imperfections at the surface are the same in both samples due to the same preparation. Because variations of the flux dynamics from different electric fields at the surface are of minor importance,[29] a comparison reflects mainly the influence of macroscopic edges on the properties of the BG. The magnetization curves of both samples in the irradiated state are very similar, as demonstrated in the inset of Fig. 9, where the moment of PI is multiplied by a factor of 9.6 for comparison with SI. The main panel of Fig. 9 shows the current density of PI vs the applied field, with the angle

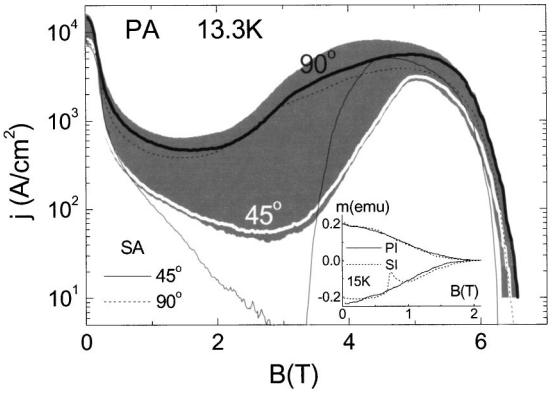

FIG. 9. Current density $j(B)$ of the V_3Si irregularly shaped crystal (*PI*) after annealing, measured for different angles Φ between crystal orientation and magnetic field *B*. The gray area covers $j(B)$ from all possible variations of Φ. If the rotation axis is parallel to the [100] direction of the crystal and *B* along [010], $j(B)$ is given by the black line ($\Phi = 90°$), whereas the white line belongs to $j(B)$ for *B* parallel to the [011] direction ($\Phi = 45°$). For comparison the corresponding results from the sphere are also shown. The magnetization of the sphere and the broken crystal, both after irradiation but before annealing are given in the inset.

Φ between the field and crystal direction as a parameter. The gray area covers all $j(B)$ values obtained at different angles. Similar to the sphere (Fig. 3), the angular dependence is present only in the BG, but its variation with Φ is smaller. It should be noticed that the angular dependence of the geometry factor in the relation $\Delta m \sim j$ is taken into account. In general the current densities in the sphere are smaller than in the piece; especially in the latter no reversible behavior is observed. We relate these differences to additional disorder induced at the macroscopic edges. The HF-O/D transitions are at slightly larger fields and less steep than in the sphere. However, if the field is directed parallel to [010] ($\Phi = 90°$ in Fig. 9) the results are quite comparable. In this geometry, where a square lattice is expected, the formation of the BG in the presence of pinning may be accompanied with disorder in excess so that the influence of edges becomes much less important. The characteristically different behavior of the BG formation, in comparing *B* parallel to [011] ($\Phi = 45°$) with [010] ($\Phi = 90°$), also exists in the irregularly shaped crystal. Edge contamination modifies the BG and the related transitions at a moderate stage at all angles except for $\Phi = 90°$, and in its vicinity. In general this conclusion may also be deduced from a comparison of the magnetic history effects. Figure 10(a) shows the strength of this metastable behavior and the related complete magnetization loops at $\Phi = 45°$ in both samples. The metastability of the BG is expected to be more pronounced in the sphere because it has no edges which serve as nuclei for the formation of the stable phase. This is in agreement with the experimental result [Fig. 10(a)]: both HEs are much more pronounced in the sphere. From the same consideration a higher value of B_{HF} and a lower value of B_{LF} are expected in SA which, however, is in contrast to the measurements. Only the fields at which the current density passes a minimum in the BG are higher in the sphere. The strength of the metastable behavior at the LF-

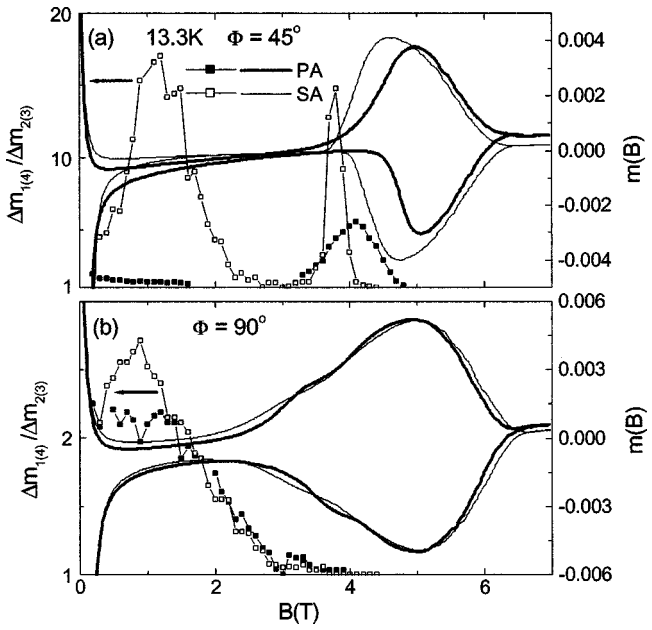

FIG. 10. Strength of the magnetic history dependence of the high-field ($\Delta m_1/\Delta m_2$) and low-field ($\Delta m_4/\Delta m_3$) order/disorder transitions and the complete magnetization loops (right axis) of the V_3Si broken crystal after annealing. (a) corresponds to the geometry magnetic field parallel to the [011], and (b) parallel to the [010] direction of the crystal. For comparison the corresponding results from the sphere are also shown, for $m(B)$ on a different scale.

O/D transition decreases in PA to values below 2, much smaller than the high-field HE but in agreement with typical measurements on irregularly shaped specimens. The reason for this different strength of the HEs between PA and SA is the mutual reduction of both effects. Due to demagnetization, the macroscopic edges in PA are assumed to be more effective in introducing disorder at the HF-O/D transition than at the LF-O/D transition. This results in an excess of disordered phases in the descending branch, which depresses the HE at the LF-O/D transition. The comparison of the HE for $\Phi = 90°$ in Fig. 10(b) shows hardly any difference between the samples: in particular the high-field HE is absent in both. This means that the correlation between the vortex and crystal lattice, which is responsible for the extraordinary behavior at this geometry, is dominating. Summarizing, contamination from macroscopic edges reduces the metastability of the vortex matter in the order/disorder transitions. This reduction is larger in the LF-O/D transition than in the HF-O/D transition. However, if the field is parallel to the [100] direction of the crystal, metastability is only present at the low-field transition and is not affected by edge contamination.

IV. SUMMARY

The formation of the Bragg glass in pure, single-crystalline V_3Si shows a strong angular dependence on the crystal orientation. For a magnetic field applied parallel to the [110] direction of the crystal, the magnetization in the Bragg glass becomes reversible, and the field region where it exists is about twice as large as for the [100] direction where a pronounced irreversible behavior is found. These characteristic differences are related to a hexagonal lattice in the first geometry and a square lattice in the latter geometry, as reported by Yethiraj *et al.*[20] The same fourfold symmetry as for the transition fields is observed in the strength of the metastable behavior of the vortex lattice. For the field parallel to [110] pronounced history effects are found for both order/disorder transitions, whereas for the [100] direction only the low-field transition is accompanied by metastability. In the latter geometry the amount of metastable disordered phase dragged from the low-field amorphous state into the Bragg glass dominates and survives up to the high-field transition. This feature prevents the usual high-field metastability, whereas apart from this direction the low-field metastability is suppressed in irregularly shaped specimens. For the angular dependence of the Bragg glass properties metastability varying with the angle between crystallographic axis and applied field remains as an alternative explanation in contrast to different vortex lattice symmetries.

ACKNOWLEDGMENT

H.K. thanks the Institut für Technische Physik, FZK for technical support and hospitality.

[1] T. Giamarchi and P. Le Doussal, Phys. Rev. Lett. **72**, 1530 (1994).
[2] D. Ertas and D. R. Nelson, Physica C **272**, 79 (1996).
[3] V. Vinokur, B. Khaykovich, E. Zeldov, M. Konczykowski, R. A. Doyle, and P. H. Kes, Physica C **295**, 1033 (1996).
[4] G. P. Mikitik and E. H. Brandt, Phys. Rev. B **64**, 184514 (2001).
[5] Y. Paltiel, E. Zeldov, Y. Myasoedov, M. L. Rappaport, G. Jung, S. Bhattacharya, M. J. Higgins, Z. L. Xiao, E. Y. Andrei, P. L. Gammel, and D. J. Bishop, Phys. Rev. Lett. **85**, 3712 (2000).
[6] Y. Paltiel, E. Zeldov, Y. Myasoedov, H. Shtrikman, S. Bhattacharya, M. J. Higgins, Z. L. Xiao, E. Y. Andrei, P. L. Gammel, and D. J. Bishop, Nature (London) **403**, 398 (2000).
[7] X. S. Ling, S. R. Park, B. A. McClain, S. M. Choi, D. C. Dender, and J. W. Lynn, Phys. Rev. Lett. **86**, 712 (2001).
[8] M. Steingart, A. G. Putz, and E. J. Kramer, J. Appl. Phys. **44**, 5580 (1973).
[9] H. Küpfer and W. Gey, Philos. Mag. **36**, 859 (1977).
[10] R. Wördenweber, P. H. Kes, and C. C. Tsuei, Phys. Rev. B **33**, 3172 (1986).
[11] S. Kokkaliaris, P. A. J. de Groot, S. N. Gordeev, A. A. Zhukov, R. Gagnon, and L. Taillefer, Phys. Rev. Lett. **82**, 5116 (1999).
[12] S. B. Roy and P. Chaddah, Physica C **279**, 70 (1997).
[13] G. Ravikumar, P. K. Mishra, V. C. Sahni, S. S. Banerjee, A. K. Grover, S. Ramakrishnan, P. L. Gammel, D. J. Bishop, E. Bucher, M. J. Higgins, and S. Battacharya, Phys. Rev. B **61**, 12 490 (2000).
[14] G. Ravikumar, H. Küpfer, A. Will, R. Meier-Hirmer, and Th. Wolf, Phys. Rev. B **65**, 094507 (2002).
[15] H. Küpfer and A. A. Manuel, Phys. Status Solidi A **54**, 153

(1979).
[16] T. Reichert, R. Meier-Hirmer, and H. Küpfer, Phys. Status Solidi A **64**, 585 (1981).
[17] R. Meier-Hirmer, H. Küpfer, and H. Scheurer, Phys. Rev. B **31**, 183 (1985).
[18] B. Obst, in *Anisotropy Effects in Superconductors*, edited by H. W. Weber (Plenum, New York, 1977), p. 139.
[19] M. R. Eskildsen, P. L. Gammel, B. P. Barber, U. Yaron, A. P. Ramirez, D. A. Huse, D. J. Bishop, C. Bolle, C. M. Lieber, S. Oxx, S. Sridhar, N. H. Andersen, K. Mortensen, and P. C. Canfield, Phys. Rev. Lett. **78**, 1968 (1996).
[20] M. Yethiraj, D. K. Christen, D. McK. Paul, P. Miranovic, and J. R. Thompson, Phys. Rev. Lett. **82**, 5112 (1999).
[21] V. G. Kogan, P. Miranovic, Lj. Dobrosavljevic-Grujic, W. E. Pickett, and D. K. Christen, Phys. Rev. Lett. **79**, 741 (1997).
[22] M. Pulver, Z. Phys. **257**, 22 (1972).
[23] A. I. Larkin and Yu. N. Ovchinnikov, J. Low Temp. Phys. **34**, 409 (1979).
[24] G. Blatter, M. V. Feigel'man, V. B. Geshkenbein, A. I. Larkin, and V. M. Vinokur, Rev. Mod. Phys. **66**, 1125 (1994).
[25] H. Küpfer, R. Meier-Hirmer, and M. Brandenbusch, in *Proceedings of the LT-17*, edited by A. Schmid, W. Weber, and H. Wühl (Elsevier, Amsterdam, 1984), CO4 (1984).
[26] S. Chaudhary, A. K. Rajarajan, K. J. Singh, S. B. Roy, and P. Chaddah, Physica C **353**, 29 (2001).
[27] G. Ravikumar, K. V. Bhagwat, V. C. Sahni, A. K. Grover, S. Ramakrishnan, and S. Bhattarcharya, Phys. Rev. B **61**, R6479 (2000).
[28] Z. L. Xiao, E. Y. Andrei, Y. Paltiel, E. Zeldov, P. Shuk, and M. Greenblatt, Phys. Rev. B **65**, 094511 (2002).
[29] H. Küpfer, A. Will, R. Meier-Hirmer, Th. Wolf, and A. A. Zhukov, Phys. Rev. B **63**, 214521 (2001).